SCIENCE CHINA
Chemistry

• ARTICLES •

September 2017 Vol.60 No.9: 1230–1235
doi: 10.1007/s11426-017-9050-6

Improving the stability of $LiNi_{0.80}Co_{0.15}Al_{0.05}O_2$ by $AlPO_4$ nanocoating for lithium-ion batteries

Ran Qi[1,2], Ji-Lei Shi[2,3], Xu-Dong Zhang[2,3], Xian-Xiang Zeng[2,3], Ya-Xia Yin[2,3], Jian Xu[2,3], Li Chen[1], Wei-Gui Fu[1*], Yu-Guo Guo[2,3*] & Li-Jun Wan[2,3]

[1]*State Key Laboratory of Separation Membranes and Membrane Processes, School of Materials Science and Engineering, Tianjin Polytechnic University, Tianjin 300071, China*
[2]*CAS Research/Education Center for Excellence in Molecular Sciences, Institute of Chemistry, Chinese Academy of Sciences, Beijing 100190, China*
[3]*School of Chemistry and Chemical Engineering, University of Chinese Academy of Sciences, Beijing 100049, China*

Received February 5, 2017; accepted April 1, 2017; published online July 18, 2017

Nickel-rich layered materials, such as $LiNi_{0.80}Co_{0.15}Al_{0.05}O_2$ (NCA), have been considered as one alternative cathode materials for lithium-ion batteries (LIBs) due to their high capacity and low cost. However, their poor cycle life and low thermal stability, caused by the electrode/electrolyte side reaction, prohibit their prosperity in practical application. Herein, $AlPO_4$ has been homogeneously coated on the surface of NCA via wet chemical method towards the target of protecting NCA from the attack of electrolyte. Compared with the bare NCA, NCA@$AlPO_4$ electrode delivers high capacity without sacrificing the discharge capacity and excellent cycling stability. After 150 cycles at 0.5 C between 3.0–4.3 V, the capacity retention of the coated material is 86.9%, much higher than that of bare NCA (66.8%). Furthermore, the thermal stability of cathode is much improved due to the protection of the uniform coating layer on the surface of NCA. These results suggest that $AlPO_4$ coated NCA materials could act as one promising candidate for next-generation LIBs with high energy density in the near future.

Li-ion batteries, cathode materials, surface modification, $AlPO_4$ coating

Citation: Qi R, Shi JL, Zhang XD, Zeng XX, Yin YX, Xu J, Chen L, Fu WG, Guo YG, Wan LJ. Improving the stability of $LiNi_{0.80}Co_{0.15}Al_{0.05}O_2$ by $AlPO_4$ nanocoating for lithium-ion batteries. *Sci China Chem*, 2017, 60: 1230–1235, doi: 10.1007/s11426-017-9050-6

1 Introduction

Lithium-ion batteries (LIBs) have been widely used as the most promising power sources in plenty of areas such as portable consumer electronics after 1990 [1,2]. Ever-increasing demand to power electric and hybrid electric vehicles has motivated intense interest in developing high-capacity electrode materials for LIBs. To obtain the high-density batteries, much research has been carried on new cathode materials with high specific capacities [3–6]. $LiNi_{0.80}Co_{0.15}Al_{0.05}O_2$ (NCA) is considered as one attractive cathode material ascribing to its high specific capacity. However, the application of NCA cathode suffers from serious challenges including the poor cyclic performance and thermal stability originating from the oxygen release during the delithiation process and the formation of NiO-like phase [7–10]. In order to overcome these problems, many research groups have proposed some effective solutions, such as surface modification, doping, core-shell [3,7,11–15]. Among these methods, the surface modification has drawn much attention because of its simple and scalable feature to realize industrialization. Although a lot of coating materials including metal oxides (e.g Al_2O_3, TiO_2), metal fluoride (AlF_3) [16–23] and $AlPO_4$ have been successfully employed to coat on the surface of cathode materials (e.g., $LiCoO_2$ [24,25], $LiNi_{1/3}Co_{1/3}Mn_{1/3}O_2$ [26],

*Corresponding authors (email: tjfwg@hotmail.com; ygguo@iccas.ac.cn)

Li-rich layered cathode materials [27]) via wet chemical procedure with the aim of enhancing the structure stability and thermal safety, to the best of our knowledge, few reports have been concentrated on coating NCA by wet chemical procedure because of its moisture sensitivity [21]. Herein, we develop a highly effective wet chemical method to realize the homogeneous $AlPO_4$ layer coating for NCA, with the aim to protect the material from the corrosion of HF and other side reactions during charging and discharging process.

NCA particles with the size of 8 μm was successfully synthesized via carbonate co-precipitation method and subsequently $AlPO_4$ layer was homogenously coated on the surface of NCA by wet chemical method [26,28–32]. After the coating process, the cycling stability of the resultant NCA@$AlPO_4$ was dramatically improved and the capacity maintains 133 mA h g^{-1} (86.9% of the initial capacity) after 150 cycles at 0.5 C rate, obviously better than that of the bare NCA (66.8%). This result indicates that the coating layer on the surface of the NCA could act as the protective layer to suppress the side reactions with the electrolyte [33]. In addition, the strong P=O bond of the coating layer could effectively enhance the thermal performance that the onset decomposition temperature of NCA@$AlPO_4$ shifts to 263.2 °C whereas that of the pristine material is 191.4 °C [34–37]. As a result, NCA@$AlPO_4$ showed better cycling life, more stable structure, and higher thermal stability than the pristine NCA material. Taking the facility into consideration, the $AlPO_4$ surface modification strategy on NCA by wet chemical synthesis shows its high effectiveness in synthesis optimization of moisture-sensitivity electrode materials and promises its wide application in other related energy storage system.

2 Experimental

2.1 Samples preparation

$LiNi_{0.80}Co_{0.15}Al_{0.05}O_2$ was synthesized by carbonate co-precipitation method [38,39]. The carbonate precursors with an appropriate amount of $LiOH{\cdot}H_2O$ (Li/(Ni+Co+Al)=1.05) were calcined at 450 °C for 6 h and 800 °C for 15 h in air, and then cooled to room temperature naturally.

To prepare $AlPO_4$ coated $LiNi_{0.80}Co_{0.15}Al_{0.05}O_2$ samples, 0.02 M of the $NH_4H_2PO_4$ powders were dissolved in 100 mL ethanol solution. The $LiNi_{0.80}Co_{0.15}Al_{0.05}O_2$ sample (2 g) was poured into the alkaline solution. Aluminum nitrate ($AlNO_3{\cdot}9H_2O$, 0.0345 g) was dissolved in ethanol solution, then slowly dropped into the above solution until the pH was within the range of 4.0–6.0. And the solution was stirred continually at 45 °C until the solvent was evaporated to obtain $AlPO_4$ coated $LiNi_{0.80}Co_{0.15}Al_{0.05}O_2$. Finally, the resulting powders were calcined at 700 °C in a muffle furnace for 10 h in air and then cooled to room temperature naturally to get the coated $LiNi_{0.80}Co_{0.15}Al_{0.05}O_2$ material.

2.2 Structural characterization

The morphology of the material was observed by scanning electron microscopy (SEM; JEOL, 6701F, Japan). X-ray diffraction (XRD) patterns of the material were conducted on a Rigaku D/max-2500 diffractometer (Philips, PW3710) with Cu Kα radiation. High-resolution transmission microscopy images (TEM; JEOL, JEM-2100F, Japan) were acquired. X-ray photoelectron spectroscopy (XPS) was performed on the Thermo Scientific ESCALab 250Xi (USA) using 200 W monochromated Al Kα radiation. Differential scanning calorimetry (DSC; NETZSCH, DSC 214, Germany) experiment was carried out at a heating rate of 10 °C min^{-1}. The delithiated cathode material (5–8 mg) and the 10 μL electrolyte in a 100 μL in the high-pressure stainless-steel DSC vessel were performed.

2.3 Electrochemical measurements

The coin-type cells were assembled in the argon atmosphere glove box and then were used to test the electrochemical performance of cathode materials. Each electrode was prepared by mixing the active powder (80 wt%), super-P acetylene black (10 wt%) and 10 wt% poly-(vinylidene fluoride) (PVDF) with the proper amount of *N*-methylpyrrolidinone (NMP). The mixed slurries were coated on Al foil and then vacuum dried at 80 °C overnight. Lithium metal and Celgard 2300 (USA) film were used respectively as the anode and separator. The electrolyte was 1 M $LiPF_6$ dissolved in the mixture of EC/DMC/DEC (1:1:1, *v*/*v*/*v*). Galvanostatic charge and discharge tests were performed by the voltage between 3.0 and 4.3 V.

3 Results and discussion

SEM and TEM images of the NCA samples and NCA@$AlPO_4$ samples were shown in Figure 1. The surface modified samples exhibit a crystalline and dense morphology (just similar to the pristine one in Figure 1(a)), and uniform size distribution. It is suggested that the micro-morphology of the NCA@$AlPO_4$ samples maintains very well after the $AlPO_4$ coating process. To visualize the detailed surface morphology, TEM characterization was carried on the NCA@$AlPO_4$ samples. TEM analysis indicates that amorphous $AlPO_4$ layer has been successfully coated on the surface of NCA with a uniform thickness of 20 nm (Figure 1(d)). This confirms the effectiveness of our wet chemical coating method on NCA particles. Subsequently, the resultant NCA@$AlPO_4$ samples were calcined at 700 °C in air to obtain the coated $LiNi_{0.80}Co_{0.15}Al_{0.05}O_2$ material. According to the prevailingly accepted viewpoint

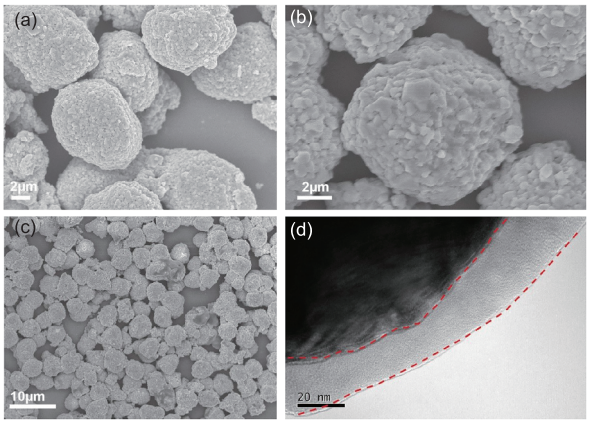

Figure 1 SEM images of the NCA samples (a) and NCA@$AlPO_4$ sample (b); (c) low magnification SEM image of the NCA@$AlPO_4$; (d) TEM image of NCA@$AlPO_4$ samples (color online).

[40], possible reactions could occur between $AlPO_4$ and cathode material substrate when heated to 700 °C. The as-obtained coating materials might belong to the amorphous lithium phosphate compounds, which are one kind of lithium-ion and electronic conductors with good electrochemical stability and thus enhance the cycling stability of cathode substrate [26,27,34]. In our work, the analysis by XPS also confirmed the existence of strong P=O bond (Figure 2). It should be noted that a peak at 133.4 eV can be seen in the P 2p spectra of the coated NCA, which can be attributed to the strong P=O bond according to the previous reports [28,35,41]. So we believed that the presentation of the coating layer on the surface of NCA could avoid the direct exposure of NCA to electrolyte, thus effectively suppresses the side reactions between them.

Figure 3 shows the Rietveld refinement of the X-ray diffraction patterns of the pure NCA material and $AlPO_4$-coated NCA material. The crystal parameters of the NCA and NCA@$AlPO_4$ material were shown in the Table 1. After coating and high temperature calcination, a small amount of Al^{3+} may be doped into the Li^+ site caused by crystal expansion. The relatively low deviation (R_{wp}=3.38%) indicates the good fit precision of as-prepared sample with the layered α-$NaFeO_2$ structure. This result clarifies that the surface modified NCA material possesses layered α-$NaFeO_2$ structure (*R*-3*m* space group). And no impurity phase is observed in the XRD patterns of the modified samples [8,42,43], indicating that the structure of the surface coated material did not change obviously compared with the bare material.

The electrochemical performances of NCA and the surface coated NCA were tested (Figure 4). Figure 4(a, b) show that the modified NCA delivers almost the same initial discharge specific capacity at 0.1 C (178 mA h g^{-1}) and rate capability as pristine NCA. Moreover, the cyclic performance of the modified samples is superior to that of pure NCA (Figure 4(c)). After 150 cycles, the discharge capacity of the modified

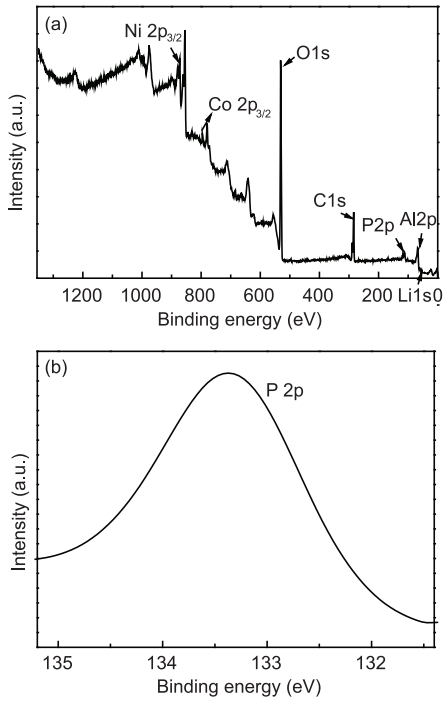

Figure 2 The elements Li, Ni, Co, Al, C, P and O from the XPS spectra of the NCA@$AlPO_4$ samples (a) and the P 2p XPS patterns of the NCA@$AlPO_4$ samples (b).

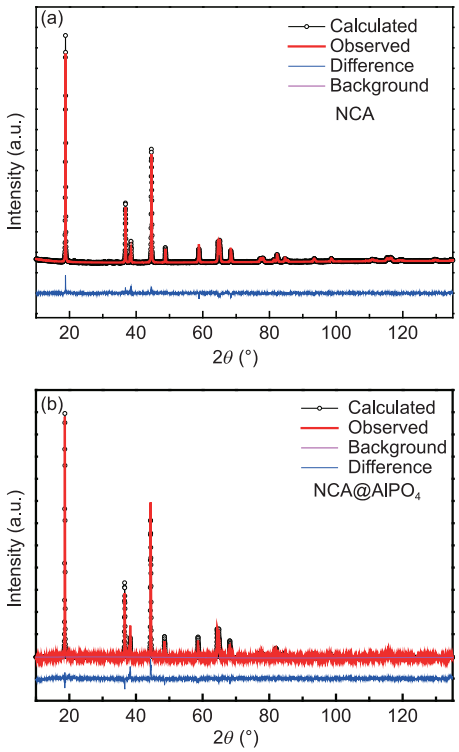

Figure 3 The Rietveld refinement of the XRD patterns of the NCA sample (a) and NCA@$AlPO_4$ sample (b) (color online).

samples maintains 133 mA h g^{-1} whereas that of the NCA declines to 103 mA h g^{-1}. In addition, the capacity retention of

Table 1 Rietveld refinement results of lattice parameter for NCA and NCA@$AlPO_4$ material

Materials	*a* (Å)	*c* (Å)	*c*/*a* ratio	Refinement parameter (%)
NCA	2.8669	14.197	4.952	R_{wp}: 2.41; R_p[a)]: 1.85
NCA@$AlPO_4$	2.8714	14.209	4.9485	R_{wp}: 3.38; R_p: 2.33

a) R_p is the residuals of the XRD patterns calculated from the model structure and the experimental data.

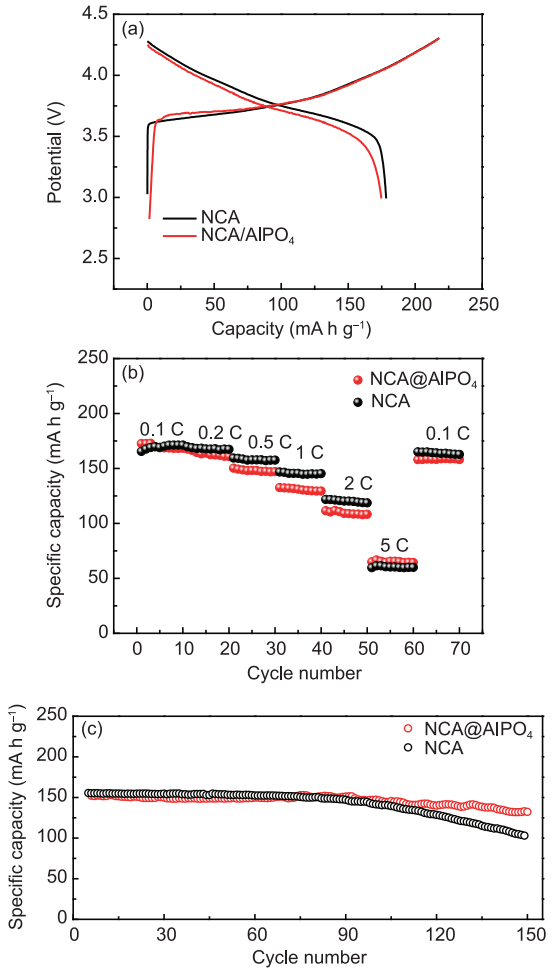

Figure 4 (a) The initial charge-discharge curves of the NCA and NCA@$AlPO_4$ material at 0.1 C; (b) the rate capability of the NCA and NCA@$AlPO_4$ material; (c) the cycling performance of the NCA and NCA@$AlPO_4$ material with voltage ranging from 3 to 4.3 V vs. Li^+/Li (color online).

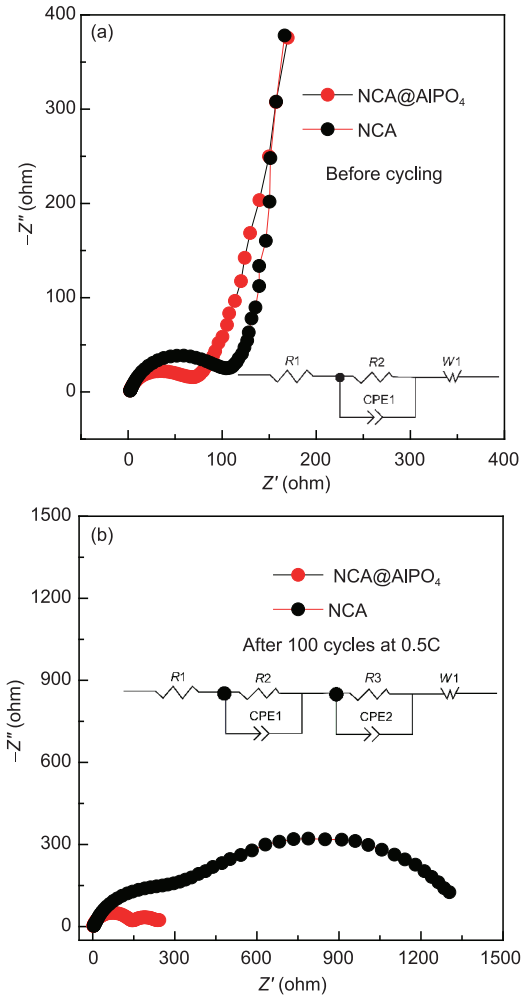

Figure 5 Electrochemical impedance spectra (EIS) of the pristine NCA and NCA@$AlPO_4$ samples before (a) and after 100 cycles (b) at 0.5 C between 3 and 4.3 V (color online).

the modified samples is 86.9%, much higher than the pristine NCA material (66.8%) at 0.5 C after 150 cycles. The much improved cycling performance of the surface coated NCA benefits from the coating layer effectively alleviating some side reactions during the charge and discharge through strong P=O bond in PO_4 poly-anion [28,36].

To reveal the inside reason for improved cycle performance of the NCA@$AlPO_4$, electrochemical impedance spectroscopy (EIS) was carried out on the pristine and modified NCA cathode. Figure 5 shows the EIS spectra of the pristine NCA and the modified samples before cycling and after 100 cycles at 0.5 C. Before cycling (Figure 5(a)), each spectrum includes a semicircle and a slope line. The intercept of the first semicircle at the high-frequency region with the real axis represents the ohmic resistance (*R*1). The semicircle at high-frequency region corresponds to the charge transfer resistance (*R*2), and the slope line at the low-frequency region is related to Warburg impedance (*W*1: the diffusion of Li^+ in the electrode). From the fitted results, the value of *R*1 (0.569 Ω) and *R*2 (51.6 Ω) of the modified sample are obviously smaller than those of the pristine (1.30 Ω, 83.7 Ω). This might come from the fact that the amorphous lithium phosphate compounds on the interface are good electrochemically

Table 2 The DSC parameters of the NCA and the NCA@$AlPO_4$

Materials	Onset temperature (°C)	Main exothermic reaction (°C)	Generated heat (J g^{-1})
NCA	191.4	280.1	1472
NCA@$AlPO_4$	263.2	284.1	1066

stable lithium-ion and electronic conductors [18,40]. After 100 cycles at 0.5 C, each spectrum exhibits two semicircles (Figure 5(b)), in which the first semicircle at high-frequency section reflects the diffusion of Li^+ through the surface layer (*R*s), and the second semicircle at low-frequency stands for the charge transfer reaction kinetics (*R*2). It can be seen that after 100 cycles at 0.5 C the modified sample shows smaller *R*2 and *R*s than the pristine sample, indicating a much better cycle stability of the modified sample. Possible reason may be that the coating layer decreases the reaction kinetics resistance and meanwhile inhibits some side reactions between cathode materials and electrolyte [27,44,45].

NCA commonly shows poor thermal instability when charged at 4.3 V [46–49]. In our case, the thermal stability of the delithiated NCA@$AlPO_4$ and pristine cathode charged at 4.3 V was conducted by differential scanning calorimetry technology (Figure 6 and Table 2). Although both two samples show sharp peaks at 280.0 °C, representing the main reaction of oxygen release and electrolyte oxidation during heating at the delithiated state, the surface modified material shows much higher onset temperature (263.2 °C) than the pristine material (191.4 °C) during the exothermal reaction. In addition, the heat generation of the modified material from the exothermal reaction is 1066 J g^{-1}, which is less than the NCA (1472 J g^{-1}) at high temperature. These results indicate that the coating materials functioned as protective layer could suppress the HF attack on NCA and reduce the oxygen release from NCA material. As expected, NCA@$AlPO_4$ cathode shows better thermal stability and reduced heat generation with regard to the NCA cathode due to the uniform protective layer [30,34,41].

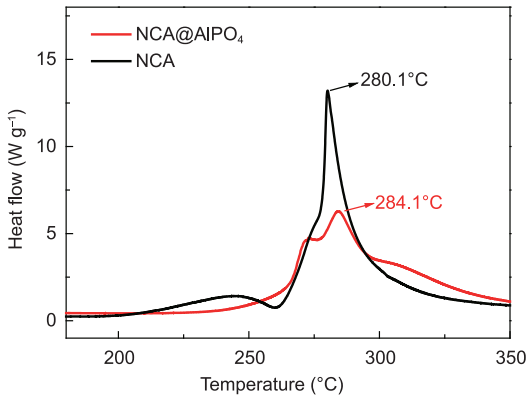

Figure 6 Differential scanning calorimetry profiles of the NCA and the NCA@$AlPO_4$ charged to 4.3 V with the electrolyte (color online).

4 Conclusions

We have successfully improved the electrochemical performances of NCA by effective $AlPO_4$ coating via the facile wet chemical procedure. With the concept of coating, the outstanding capacity retention of 86.9% is obtained for the surface modified NCA after 150 cycles at 0.5 C. Additionally, the modified sample shows much better thermal stability and smaller ohmic resistance as well as charge transfer resistance value. The results indicate that the coating materials derived from $AlPO_4$ can act as a stable layer to protect the active material and suppress side reactions between NCA and the electrolyte. Therefore, $AlPO_4$ coating layer to modify the sample surface is a viable method to improve the cycling performance and thermal stability of NCA. Moreover, these results will open new options to improve the properties of other related electrode materials for rechargeable batteries in the near future.

Acknowledgments This work was supported by the National Natural Science Foundation of China (21303222, 21127901, 51303132), the National Key Research and Development Program of China (2016YFA0202500), and the 'Strategic Priority Research Program' of the Chinese Academy of Sciences (XDA09010100).

Conflict of interest The authors declare that they have no conflict of interest.

1 Goodenough JB, Park KS. *J Am Chem Soc*, 2013, 135: 1167–1176
2 Guo YG, Hu JS, Wan LJ. *Adv Mater*, 2008, 20: 2878–2887
3 Nitta N, Wu F, Lee JT, Yushin G. *Mater Today*, 2015, 18: 252–264
4 Choi NS, Chen Z, Freunberger SA, Ji X, Sun YK, Amine K, Yushin G, Nazar LF, Cho J, Bruce PG. *Angew Chem Int Ed*, 2012, 51: 9994–10024
5 Ma J, Hu P, Cui G, Chen L. *Chem Mater*, 2016, 28: 3578–3606
6 Zhang J, Guo X, Yao S, Qiu X. *Sci China Chem*, 2016, 59: 1479–1485
7 Lim BB, Yoon SJ, Park KJ, Yoon CS, Kim SJ, Lee JJ, Sun YK. *Adv Funct Mater*, 2015, 25: 4673–4680
8 Makimura Y, Sasaki T, Nonaka T, Nishimura YF, Uyama T, Okuda C, Itou Y, Takeuchi Y. *J Mater Chem A*, 2016, 4: 8350–8358
9 Kim H, Lee S, Cho H, Kim J, Lee J, Park S, Joo SH, Kim SH, Cho YG, Song HK, Kwak SK, Cho J. *Adv Mater*, 2016, 28: 4705–4712
10 Kleiner K, Dixon D, Jakes P, Melke J, Yavuz M, Roth C, Nikolowski K, Liebau V, Ehrenberg H. *J Power Sources*, 2015, 273: 70–82
11 Wang Y, Cao G. *Adv Mater*, 2008, 20: 2251–2269
12 Park BC, Bang HJ, Amine K, Jung E, Sun YK. *J Power Sources*, 2007, 174: 658–662
13 Li C, Zhang HP, Fu LJ, Liu H, Wu YP, Rahm E, Holze R, Wu HQ. *Electrochim Acta*, 2006, 51: 3872–3883
14 Zhu C, Yu Y, Gu L, Weichert K, Maier J. *Angew Chem Int Ed*, 2011,

50: 6278–6282
15 Cao AM, Hu JS, Wan LJ. *Sci China Chem*, 2012, 55: 2249–2256
16 Wang F, Xiao S, Chang Z, Li M, Wu Y , Holze R. *Int J Electrochem Sci*, 2014, 9: 6182–6190
17 Zhao J, Qu G, Flake JC, Wang Y. *Chem Commun*, 2012, 48: 8108–8110
18 Wang KX, Li XH, Chen JS. *Adv Mater*, 2015, 27: 527–545
19 Wang F, Xiao S, Li M, Wang X, Zhu Y, Wu Y, Shirakawa A, Peng J. *J Power Sources*, 2015, 287: 416–421
20 Lee SH, Yoon CS, Amine K, Sun YK. *J Power Sources*, 2013, 234: 201–207
21 Zhu L, Liu Y, Wu W, Wu X, Tang W, Wu Y. *J Mater Chem A*, 2015, 3: 15156–15162
22 Lee DJ, Scrosati B, Sun YK. *J Power Sources*, 2011, 196: 7742–7746
23 Shi Y, Zhang M, Qian D, Meng YS. *Electrochim Acta*, 2016, 203: 154–161
24 Quinlan RA, Lu YC, Kwabi D, Shao-Horn Y, Mansour AN. *J Electrochem Soc*, 2016, 163: A300–A308
25 Cho J, Lee JG, Kim B, Park B. *Chem Mater*, 2003, 15: 3190–3193
26 Wang JH, Wang Y, Guo YZ, Ren ZY, Liu CW. *J Mater Chem A*, 2013, 1: 4879–4884
27 Wu F, Zhang X, Zhao T, Li L, Xie M, Chen R. *ACS Appl Mater Interfaces*, 2015, 7: 3773–3781
28 Yang FL, Zhang W, Chi ZX, Cheng FQ, Chen JT, Cao AM, Wan LJ. *Chem Commun*, 2015, 51: 2943–2945
29 Huang X, Qiao Q, Sun Y, Li F, Wang Y, Ye S. *J Solid State Electrochem*, 2014, 19: 805–812
30 Shi JY, Yi CW, Kim K. *J Power Sources*, 2010, 195: 6860–6866
31 Liu J, Manthiram A. *Chem Mater*, 2009, 21: 1695–1707
32 Cho J, Kim YW, Kim B, Lee JG, Park B. *Angew Chem Int Ed*, 2003, 42: 1618–1621
33 Oh P, Song B, Li W, Manthiram A. *J Mater Chem A*, 2016, 4: 5839–5841
34 Lee KT, Jeong S, Cho J. *Acc Chem Res*, 2013, 46: 1161–1170
35 Li JF, Huang YF, Ding Y, Yang ZL, Li SB, Zhou XS, Fan FR, Zhang W, Zhou ZY, Wu DY, Ren B, Wang ZL, Tian ZQ. *Nature*, 2010, 464: 392–395
36 Lu YC, Mansour AN, Yabuuchi N, Shao-Horn Y. *Chem Mater*, 2009, 21: 4408–4424
37 Cho W, Kim SM, Lee KW, Song JH, Jo YN, Yim T, Kim H, Kim JS, Kim YJ. *Electrochim Acta*, 2016, 198: 77–83
38 Jo M, Noh M, Oh P, Kim Y, Cho J. *Adv Energy Mater*, 2014, 4: 1301583
39 Lee MH, Kang YJ, Myung ST, Sun YK. *Electrochim Acta*, 2004, 50: 939–948
40 Liu W, Oh P, Liu X, Lee MJ, Cho W, Chae S, Kim Y, Cho J. *Angew Chem Int Ed*, 2015, 54: 4440–4457
41 Appapillai AT, Mansour AN, Cho J, Shao-Horn Y. *Chem Mater*, 2007, 19: 5748–5757
42 Cho SW, Kim GO, Ju JH, Oh JW, Ryu KS. *Mater Res Bull*, 2012, 47: 2830–2833
43 Robert R, Bünzli C, Berg EJ, Novák P. *Chem Mater*, 2015, 27: 526–536
44 Bian X, Fu Q, Qiu H, Du F, Gao Y, Zhang L, Zou B, Chen G, Wei Y. *Chem Mater*, 2015, 27: 5745–5754
45 Cho Y, Oh P, Cho J. *Nano Lett*, 2013, 13: 1145–1152
46 Nam KW, Bak SM, Hu E, Yu X, Zhou Y, Wang X, Wu L, Zhu Y, Chung KY, Yang XQ. *Adv Funct Mater*, 2013, 23: 1047–1063
47 Kalyani P, Kalaiselvi N. *Sci Tech Adv Mater*, 2005, 6: 689–703
48 Guilmard M, Croguennec L, Delmas C. *Chem Mater*, 2003, 15: 4484–4493
49 Belharouak I, Lu W, Liu J, Vissers D, Amine K. *J Power Sources*, 2007, 174: 905–909